Inorg. Chem. **2005**, *44*, 8125–8134

Non-heme Iron(II) Complexes Containing Tripodal Tetradentate Nitrogen Ligands and Their Application in Alkane Oxidation Catalysis

George J. P. Britovsek,* Jason England, and Andrew J. P. White

Department of Chemistry, Imperial College London, Exhibition Road, London, SW7 2AY, U.K.

Received June 8, 2005

A series of iron(II) bis(triflate) complexes containing tripodal tetradentate nitrogen ligands with pyridine and dimethylamine donors of the type $[N(CH_2Pyr)_{3-n}(CH_2CH_2NMe_2)_n]$ [$n = 0$ (tpa, **1**), $n = 1$ (*iso*-bpmen, **3**), $n = 2$ (Me_4-benpa, **4**), $n = 3$ (Me_6-tren, **5**)] and the linear tetradentate ligand $[(CH_2Pyr)MeN(CH_2CH_2)NMe(CH_2Pyr)$, (bpmen, **2**)] has been prepared. The preferred coordination geometry of these complexes in the solid state and in CH_2Cl_2 solution changes from six- to five-coordinate in the order from **1** to **5**. In acetonitrile, the triflate ligands of all complexes are readily displaced by acetonitrile ligands. The complex $[Fe(\mathbf{1})(CH_3CN)_2]^{2+}$ is essentially low spin at room temperature, whereas ligands with fewer pyridine donors increase the preference for high-spin Fe(II). Both the number of pyridine donors and the spin state of the metal center strongly affect the intensity of a characteristic MLCT band around 400 nm. The catalytic properties of the complexes for the oxidation of alkanes have been evaluated, using cyclohexane as the substrate. Complexes containing ligands **1**–**3** are more active and selective catalysts, possibly operating via a metal-based oxidation mechanism, whereas complexes containing ligands **4** and **5** give rise to Fenton-type chemistry.

Introduction

Light alkanes are notoriously difficult to functionalize selectively and are therefore currently underused as a chemical feedstock. The largest industrial application of alkanes in chemical synthesis is currently the steam reforming process, which converts methane into syngas (CO/H_2). The direct selective oxidation of methane to methanol, which would be of immense industrial interest,[1] has not been achieved on an industrial scale thus far, despite considerable research effort, both in industry and academia.[2,3] Some successes in the selective oxidation of other hydrocarbons have been achieved, for example the Mid-Century/Amoco oxidation process of *p*-xylene to terephthalic acid[4] and the oxidation of cyclohexane to a mixture of cyclohexanol and cyclohexanone.[5] Both processes are carried out in a homogeneous phase using transition metal catalysts based on manganese or cobalt. With the advent of large-scale gas-to-liquid (GTL) processing,[6] higher alkanes will become available in ever increasing amounts and the future efficient utilization of this carbon resource will depend on the development of highly active, selective and stable oxidation catalysts.[7−9]

During the past decade, it has emerged that non-heme iron-based catalysts show great potential for the selective oxidation of alkanes.[10,11] Some of these catalysts have shown unusually high activities and product selectivities distinct from the typical product distributions obtained by Fenton-

* To whom correspondence should be addressed. Tel: +44-(0)20-75945863. Fax: +44-(0)20-75945804. E-mail: g.britovsek@imperial.ac.uk.

(1) Lange, J.-P. *Ind. Eng, Chem. Res.* **1997**, *36*, 4282−4290.
(2) Sheldon, R. A.; Kochi, J. K. *Metal-Catalyzed Oxidations of Organic Compounds*; Academic Press: New York, 1981.
(3) Shilov, A. E.; Shul'pin, G. B. *Activation and Catalytic Reactions of Saturated Hydrocarbons in the Presence of Metal Complexes*; Kluwer: Dordrecht, 2000.
(4) Partenheimer, W. *Catal. Today* **1995**, *23*, 69−158.
(5) Ingold, K. U. *Aldrichimica Acta* **1989**, *22*, 69−73.
(6) Wilhelm, D. J.; Simbeck, D. R.; Karp, A. D.; Dickenson, R. L. *Fuel Proc. Technol.* **2001**, *71*, 139−148.
(7) Arakawa, H.; Aresta, M.; Armor, J. N.; Barteau, M. A.; Beckman, E. J.; Bell, A. T.; Bercaw, J. E.; Creutz, C.; Dinjus, E.; Dixon, D. A.; Domen, K.; DuBois, D. L.; Eckert, J.; Fujita, E.; Gibson, D. H.; Goddard, W. A.; Goodman, D. W.; Keller, J.; Kubas, G. J.; Kung, H. H.; Lyons, J. E.; Manzer, L. E.; Marks, T. J.; Morokuma, K.; Nicholas, K. M.; Periana, R. A.; Que, L., Jr.; Rostrup-Nielson, J.; Sachtler, W. M. H.; Schmidt, L. D.; Sen, A.; Somorjai, G. A.; Stair, P. C.; Stults, B. R.; Tumas, W. *Chem. Rev.* **2001**, *101*, 953−996.
(8) Labinger, J. A. *J. Mol. Catal.* **2004**, *220*, 27−35.
(9) Periana, R. A.; Bhalla, G.; Tenn, W. J., III; Young, K. J. H.; Liu, X. Y.; Mironov, O.; Jones, C. J.; Ziatdinov, V. R. *J. Mol. Catal.* **2004**, *220*, 7−25.
(10) Costas, M.; Mehn, M. P.; Jensen, M. P.; Que, L., Jr. *Chem. Rev.* **2004**, *104*, 939−986.
(11) Costas, M.; Chen, K.; Que, L., Jr. *Coord. Chem. Rev.* **2000**, *200*−*202*, 517−544.

10.1021/ic0509229 CCC: $30.25
Published on Web 09/29/2005

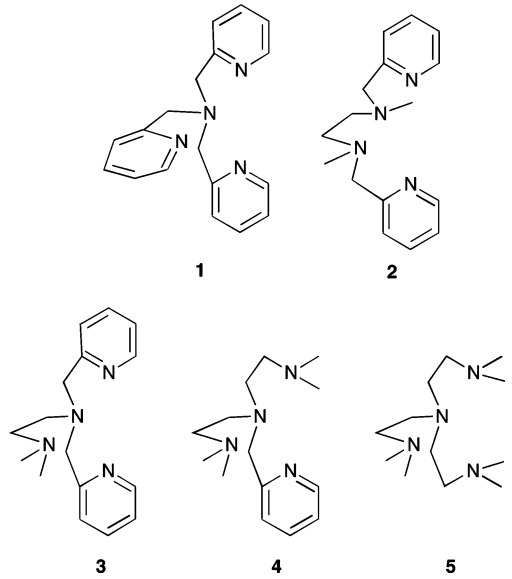

Figure 1. Tetradentate ligands containing pyridine and amine donors.

type oxidations.[12,13] For example, cyclohexane is oxidized by H_2O_2 to give cyclohexanol as the major product when a catalytic amount of an iron(II) complex containing the tetradentate tris(pyridylmethyl)amine ligand (tpa, **1**, Figure 1) is used.[14,15] Another complex, $[Fe(\mathbf{2})(CH_3CN)_2][ClO_4]_2$, containing the tetradentate bis(pyridylmethyl)ethylenediamine ligand (bpmen, **2**), has shown even better catalytic efficiency.[16] Oxygen- and deuterium-labeling studies have established that, unlike in Fenton chemistry, O_2 is not involved in these oxidations.[16] In addition, stereospecific hydroxylation has been observed with a prochiral substrate.[17,18] These observations have led to the conclusion that alkane hydroxylation reactions, catalyzed by non-heme iron(II) complexes with ligands such as **1** and **2**, occur via a different mechanism from unselective radical chain autooxidation (Fenton chemistry)[19] and a mechanism based on high valent iron(IV) or iron(V) oxo species has been invoked.[10] Although already proposed in 1932,[20] the existence of such high-valent iron-oxo species as an intermediate has gained strong support recently through the first crystallographic characterization of two non-heme Fe(IV) oxo complexes.[21]

These promising advances in selective alkane oxidation have led us to initiate a research program to investigate the catalytic properties of iron(II) bis(triflate) complexes containing multidentate nitrogen ligands with the aim to increase the understanding of the factors that are important for catalytic activity and selectivity and to improve on catalyst efficiency, i.e., activity, selectivity, and stability. In a previous report, iron(II) complexes containing tridentate bis(imino)pyridine and bis(amino)pyridine ligands have been investigated as catalysts for the oxidation of cyclohexane.[22] Only low activities and selectivities were obtained with these complexes, indicative of Fenton-type chemistry. Here we report our investigations regarding the effect of pyridyl versus amine donors in tpa-type catalysts. Thus, a series of new iron(II) bis(triflate) complexes has been prepared containing tripodal tetradentate nitrogen ligands where the pyridyl donors of tpa are successively replaced by dimethylamine donors to give the ligands *iso*-bpmen (**3**), Me_4-benpa (**4**), and Me_6-tren (**5**) (Figure 1). The coordination geometry, solution behavior, and electronic properties of these complexes have been studied by NMR and UV−vis spectroscopy and X-ray analysis. The catalytic properties for the oxidation of cyclohexane with H_2O_2 have been evaluated and directly compared with the parent tpa (**1**) and bpmen (**2**) iron triflate complexes.

Results and Discussion

Ligand and Complex Synthesis. The reported synthetic procedures for the pyridylamine ligands tpa (**1**),[23,24] bpmen (**2**),[25,26] and *iso*-bpmen (**3**)[27] were found to be rather tedious, and yields were moderate at best in our hands. We therefore devised alternative procedures for these ligands by reductive amination of pyridine carboxaldehyde, using sodium triacetoxyborohydride as the reducing agent (Scheme 1). This method is not only much more convenient and gives higher yields compared to the previously reported procedures, but it also avoids the use of the severe irritant picolyl chloride. The new compound bis(dimethylaminoethyl)pyridylmethylamine (Me_4-benpa, **4)** was prepared via a similar protocol, using *N*,*N*,*N*′,*N*′-tetramethyldiethylene triamine. Tris(2-dimethylaminoethyl)amine (Me_6-tren, **5**), previously prepared by reductive methylation of tren,[28] was more conveniently prepared using sodium borohydride instead of formic acid as the reducing agent.

The synthesis of complex $[Fe(\mathbf{1})OTf_2]$ has been reported previously.[29] Complex $[Fe(\mathbf{2})OTf_2]$ has been used recently in oxidation catalysis, but no synthetic procedure nor characterization was reported.[30] We have prepared complexes $[Fe(\mathbf{2})OTf_2]$ and $[Fe(\mathbf{3})OTf_2]$ by combining the ligands bpmen (**2**) and iso-bpmen (**3)** with $Fe(OTf)_2(CH_3CN)_2$ in

(12) Walling, C. *Acc. Chem. Res.* **1975**, *8*, 125−131.
(13) Sawyer, D. T. *Coord. Chem. Rev.* **1997**, *165*, 297−313.
(14) Kim, J.; Harrison, R. G.; Kim, C.; Que, L., Jr. *J. Am. Chem. Soc.* **1996**, *118*, 4373−4379.
(15) Lim, M. H.; Rohde, J.-U.; Stubna, A.; Bukowski, M. R.; Costas, M.; Ho, R. Y. N.; Münck, E.; Nam, W.; Que, L., Jr. *PNAS* **2003**, *100*, 3665−3670.
(16) Chen, K.; Que, L., Jr. *Chem. Commun.* **1999**, 1375−1376.
(17) Kim, C.; Chen, K.; Kim, J.; Que, L., Jr. *J. Am. Chem. Soc.* **1997**, *119*, 5964−5965.
(18) Chen, K.; Que, L., Jr. *J. Am. Chem. Soc.* **2001**, *123*, 6327−6337.
(19) Gozzo, F. *J. Mol. Catal.* **2001**, *171*, 1−22.
(20) Bray, W. C.; Gorin, M. H. *J. Am. Chem. Soc.* **1932**, *54*, 2124−2125.
(21) (a) Rohde, J.-U.; In, J.-H.; Lim, M. H.; Brennessel, W. W.; Bukowski, M. R.; Stubna, A.; Münck, E.; Nam, W.; Que, L., Jr. *Science* **2003**, *299*, 1037−1039. (b) Klinker, E. J.; Kaizer, J.; Brennessel, W. W.; Woodrum, N. L.; Cramer, C. J.; Que, L., Jr. *Angew. Chem., Int. Ed.* **2005**, *44*, 3690−3694.
(22) Britovsek, G. J. P.; England, J.; Spitzmesser, S. K.; White, A. J. P.; Williams, D. J. *Dalton Trans.* **2005**, 945−955.
(23) Anderegg, G.; Wenk, F. *Helv. Chim. Acta* **1967**, *50*, 2330−2332.
(24) Canary, J. W.; Wang, Y.; Roy Jr., R. *Inorg. Synth.* **1998**, *32*, 70−75.
(25) Toftlund, H.; Pedersen, E.; Yde-Andersen, S. *Acta Chem. Scand.* **1984**, *38A*, 693−697.
(26) Che, C.-M.; Tang, W. T.; Wong, W. T.; Wong, K. Y.; Lai, T. F. *J. Chem. Res., Synop.* **1991**, 30.
(27) Weitzer, M.; Schatz, M.; Hampel, F.; Heinemann, F. W.; Schindler, S. *J. Chem. Soc., Dalton Trans.* **2002**, 686−694.
(28) Ciampolini, M.; Nardi, N. *Inorg. Chem.* **1966**, *5*, 41−44.
(29) Diebold, A.; Hagen, K. S. *Inorg. Chem.* **1998**, *37*, 215−223.
(30) Fujita, M.; Que, L., Jr. *Adv. Synth. Catal.* **2004**, *346*, 190−194.

Scheme 1

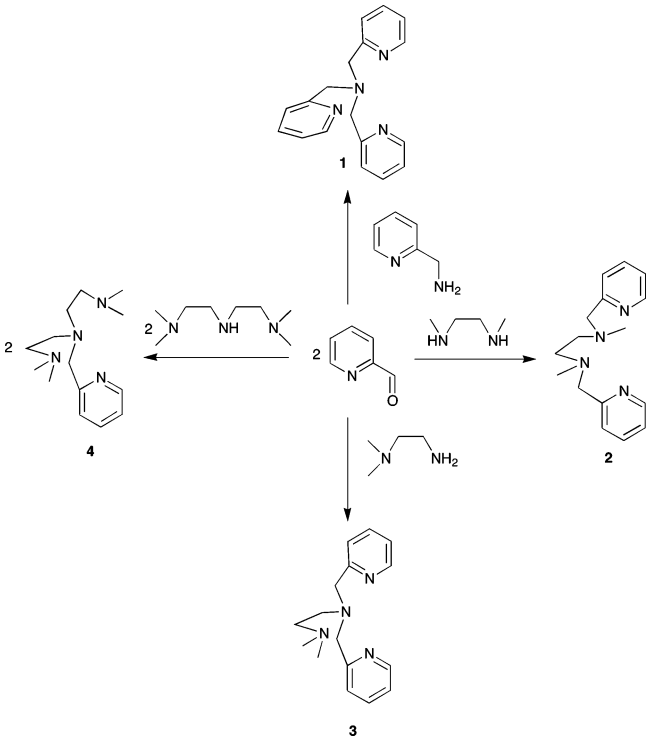

Scheme 2

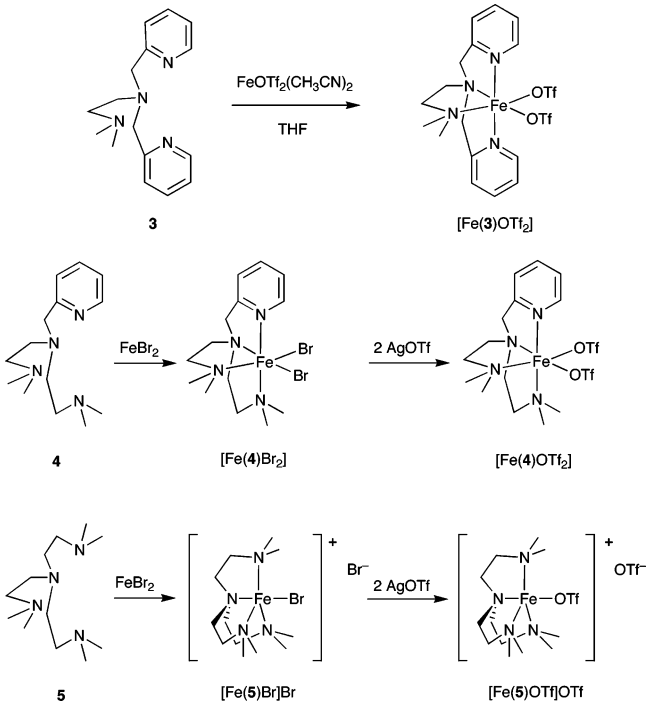

tetrahydrofuran and the complexes have been obtained as yellow solids in good yield (Scheme 2). The same procedure did not work for the reaction of ligands **4** and **5** with Fe(OTf)$_2$(CH$_3$CN)$_2$, and a two-step route via the iron(II) dibromo complex [Fe(**4**)Br$_2$] and [Fe(**5**)Br]Br[31,32] had to be devised. Subsequent reaction with 2 equiv of AgOTf yields the complexes [Fe(**4**)OTf$_2$] and [Fe(**5**)OTf$_2$]. All complexes are stable in the solid state when stored under nitrogen at room temperature, except [Fe(**4**)OTf$_2$], which decomposes slowly within one month. All complexes have been characterized by ^{1}H and ^{19}F NMR and UV−vis spectroscopy, mass spectrometry, elemental analysis, and magnetic moment. In addition, complexes [Fe(**3**)OTf$_2$] and [Fe(**5**)OTf$_2$] have been analyzed by X-ray diffraction.

Solution Behavior. The coordination chemistry of tripodal nitrogen ligands such as tpa and tren has been recently reviewed.[33] The relatively complicated solution behavior of complex [Fe(**1**)OTf$_2$] in various solvents has been thoroughly investigated by Hagen and Diebold.[29] It was found that in noncoordinating solvents such as CDCl$_3$, [Fe(**1**)OTf$_2$] is paramagnetic at 298 K. The equivalence of all three pyridylmethyl moieties in the ^{1}H NMR spectrum is believed to be due to a fast exchange between a six-coordinate and a five-coordinate complex with effective 3-fold symmetry, as shown in eq 1. Our ^{19}F NMR spectroscopic studies confirm this picture.

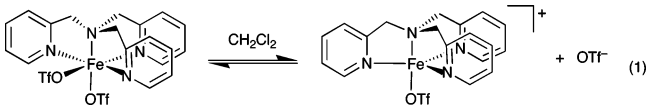

(1)

^{19}F NMR spectroscopy is particularly useful for determining whether triflate anions are coordinated to a metal center. In diamagnetic compounds, the ^{19}F chemical shift for a triflate group in CD$_2$Cl$_2$ at room temperature can vary between −78.7 ppm for a covalently bound triflate in Me$_3$SiOTf[34] and −80.5 ppm for ionic triflate in [PPN]OTf (PPN = Ph$_3$P=N=PPh$_3^+$).[35] Diamagnetic transition metal triflate complexes also generally show ^{19}F resonances between −77 and −79 ppm.[36] In paramagnetic iron(II) complexes, much larger differences in chemical shifts are observed, ranging from ca. +60 (bridging triflate) to ca. −10 (terminal) and ca. −80 ppm (free triflate).[37,38] The ^{19}F NMR spectrum of [Fe(**1**)OTf$_2$] in CD$_2$Cl$_2$ shows one single peak at −21 ppm, which indicates that the triflate ligands are predominantly coordinated. As only one slightly broadened ($\nu_{1/2}$ = 179 Hz) peak is observed, a relatively fast exchange as shown in eq 1 must occur, rendering both triflate ligands equivalent on the NMR time scale (Table 1).

In CD$_3$CN at 298 K, the ^{1}H NMR spectrum of [Fe(**1**)OTf$_2$] is nearly diamagnetic and the solution magnetic moment $\mu_{eff} = 0.98\mu_B$. In this solvent, the exchange process is potentially more complicated due to a competition between CD$_3$CN and the triflate anions. A single ^{19}F NMR resonance is observed at −78 ppm, which suggests that the triflate anions are not coordinated. This peak is relatively sharp ($\nu_{1/2}$

(31) Ciampolini, M.; Nardi, N. *Inorg. Chem.* **1966**, *5*, 1150−1154.
(32) Di Vaira, M.; Orioli, P. L. *Acta Crystallogr.* **1968**, *B24*, 1269−1272.
(33) Blackman, A. G. *Polyhedron* **2005**, *24*, 1−39.
(34) Jones, V. A.; Sriprang, S.; Thornton-Pett, M.; Kee, T. P. *J. Organomet. Chem.* **1998**, *567*, 199−218.
(35) Burger, P.; Baumeister, J. M. *J. Organomet. Chem.* **1999**, *575*, 214−222.
(36) Mahon, M. F.; Whittlesey, M. K.; Wood, P. T. *Organometallics* **1999**, *18*, 4068−4074.
(37) Blakesley, D. W.; Payne, S. C.; Hagen, K. S. *Inorg. Chem.* **2000**, *39*, 1979−1989.
(38) Börzel, H.; Comba, P.; Hagen, K. S.; Lampeka, Y. D.; Lienke, A.; Linti, G.; Merz, M.; Pritzkow, H.; Tsymbal, L. V. *Inorg. Chim. Acta* **2002**, *337*, 407−419.

Table 1. Selected Physical Parameters of Iron Bis(triflate) Complexes

	^{19}F CD_2Cl_2		^{19}F CD_3CN					
complex	δ (ppm)	$\nu_{1/2}$ (Hz)	δ (ppm)	$\nu_{1/2}$ (Hz)	λ_{max}[a] (nm)	ϵ_{max}[a] (M^{-1} cm^{-1})	μ_{eff}[b] CD_2Cl_2 (μ_B)	μ_{eff}[b] CD_3CN (μ_B)
[Fe(**1**)OTf_2]	−21	179	−78	12	399	5700	5.16	0.98
[Fe(**2**)OTf_2]	−29	716	−77	845	375	3800	5.27	4.26
[Fe(**3**)OTf_2]	−24	1330	−66	920	374	1100	5.32	4.72
[Fe(**4**)OTf_2]	−44	4848	−68	358	−	−	4.89	4.89
[Fe(**5**)OTf]OTf	18, −78	118, 47	−78	205	−	−	4.92	nd

[a] c = 0.5 mM in CH_3CN. [b] Evans' NMR method, 298 K.

= 12 Hz), which is probably due to a slow exchange (if any) between triflate and acetonitrile and possibly also due to the low magnetic moment. Thus, the major species in CD_3CN solution is the diamagnetic bis(acetonitrile) complex [Fe(**1**)$(CD_3CN)_2]^{2+}$.

Complex [Fe(**2**)OTf_2] is high spin in CD_2Cl_2 at 298 K (μ_{eff} = 5.16μ_B), and the ^{1}H NMR spectrum shows the expected signals between 170 and −16 ppm. In CD_3CN, the peaks are severely broadened at 298 K and interpretation of the spectrum is not straightforward. The ^{1}H NMR spectrum of the related, previously reported,[39] complex [Fe(**2**)$(CH_3CN)_2](ClO_4)_2$ was recorded for comparison and shows much sharper signals under the same conditions. This surprising anion effect on line broadening is attributed to the nature of the anion affecting the exchange processes between coordinated and free anions and acetonitrile molecules. The ^{19}F NMR spectrum of [Fe(**2**)OTf_2] in CD_2Cl_2 shows a single broad peak at −29 ppm ($\nu_{1/2}$ = 716 Hz). Although both coordinated triflate anions are equivalent in this case, the severe line broadening indicates a fast exchange between coordinated and free triflate anions, similar to eq 1. In CD_3CN, also one broad peak is observed at −77 ppm, suggesting that the main species is the [Fe(**2**)$(CH_3CN)_2]^{2+}$ cation. This species displays a much larger magnetic moment in CD_3CN (μ_{eff} = 4.26μ_B at 298 K) compared to [Fe(**1**)$(CD_3CN)_2]^{2+}$. It has been shown previously that cooling a solution of [Fe(**2**)$(CH_3CN)_2](ClO_4)_2$ to −40 °C induces a spin crossover.[39] Similar to the bis(triflate) complexes being in equilibrium with a five-coordinate mono(triflate) species (as in eq 1), bis(acetonitrile) complexes can also be in equilibrium with a mono(acetonitrile) species, which will have a different magnetic moment, and this equilibrium will be temperature dependent. A deconvolution of the exchange versus spin crossover processes for [Fe(**2**)$(CH_3CN)_2](ClO_4)_2$ was recently reported by Bryliakov and co-workers.[40]

Replacing one pyridylmethyl moiety in complex [Fe(**1**)OTf_2] by a dimethylaminoethyl group, as in [Fe(**3**)OTf_2] results in a severe line broadening in the ^{19}F NMR spectra (see Table 1). The ^{19}F NMR spectrum in CD_2Cl_2 shows a very broad resonance at −24 ppm, again indicating exchange between coordinated and uncoordinated triflate anions, whereas in CD_3CN a single broad signal at −66 ppm is seen, showing that [Fe(**3**)$(CH_3CN)_2]^{2+}$ is still the major species in solution. The complexity of the solution behavior has increased in this case as the 3-fold symmetry is lost, giving rise to additional isomers that can exist in solution, as shown in eq 2. Cooling a solution of [Fe(**3**)OTf_2] in CD_3CN down

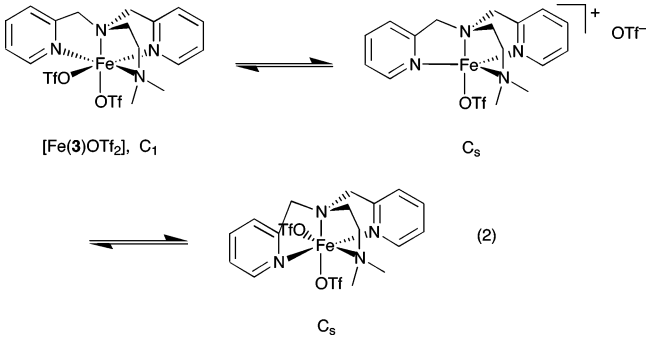

to −40 °C does decrease the chemical shift range, but the severe line broadening prevents any meaningful interpretation. The magnetic moment is very close to the expected spin-only value (μ_{eff} = 4.72μ_B at 298 K), and any spin crossover is likely to be at a much lower temperature.

The replacement of another pyridylmethyl by a dimethylaminoethyl moiety, complex [Fe(**4**)OTf_2], results in a further broadening of the ^{19}F NMR signal in CD_3CN at −68 ppm, whereas in CD_2Cl_2, an extremely broad peak around 44 ppm can be observed (see Table 1). Finally, the tris(dimethylaminoethyl)amine complex [Fe(**5**)OTf_2] shows a different solution behavior compared to that of the complexes of **1**−**4**. The ^{1}H NMR spectrum of [Fe(**5**)OTf_2] at room temperature in CD_3CN or CD_2Cl_2 is too broad for meaningful interpretation. The ^{19}F NMR spectrum in CD_2Cl_2 on the other hand shows two sharp peaks, one at −78 and one at +18 ppm, indicating one uncoordinated triflate anion and one bound to the iron(II) center and that their exchange is slow or does not occur. It appears thus that the equilibrium between six- and five-coordinate species, similar as in eq 1, lies predominantly on the right-hand side in his case. In CD_3CN, only uncoordinated triflate is observed (one peak at −78 ppm), indicating that an acetonitrile complex has been formed, probably a mono(acetonitrile) complex [Fe(**5**)$(CD_3CN)]^{2+}$.

UV−Vis Spectroscopy. The visible region of the electronic spectra of the complexes [Fe(**1**)OTf_2], [Fe(**2**)OTf_2], and [Fe(**3**)OTf_2] in acetonitrile solution is dominated by an intense band around 400 nm (see Figure 2). This band is due to a metal-to-ligand charge transfer process (MLCT), which has been previously observed for other iron(II) complexes containing pyridine-based ligands.[29,41−44] The λ_{max} values reported in Table 1 for [Fe(**1**)OTf_2] and [Fe(**2**)OTf_2] are comparable to those reported previously for [Fe(**1**)OTf_2]

(39) Chen, K.; Costas, M.; Kim, J.; Tipton, A.; Que, L., Jr. *J. Am. Chem. Soc.* **2002**, *124*, 3026−3035.
(40) Bryliakov, K. P.; Duban, E. A.; Talsi, E. P. *Eur. J. Inorg. Chem.* **2005**, 72−76.

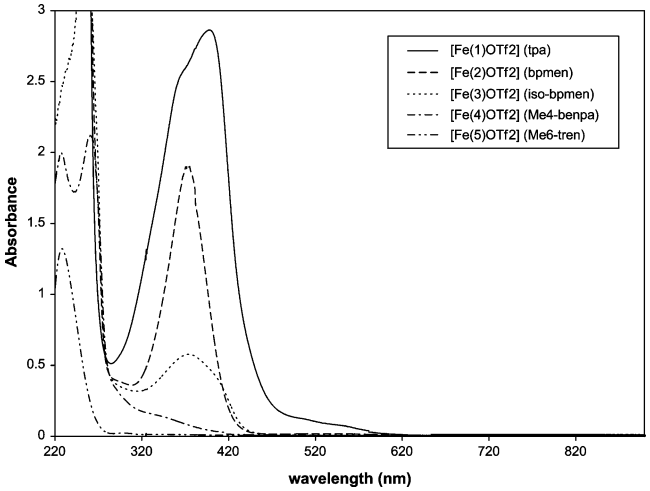

Figure 2. UV−vis spectra of iron(II) bistriflate complexes in acetonitrile (c = 0.5 mM).

(λ_{max}= 399 nm, ϵ_{max}= 8611 M^{-1} cm^{-1})[29] and for the related complex [Fe(**2**)$(CH_3CN)_2$]$(SbF_6)_2$ (λ_{max}= 373 nm, ϵ_{max}= 5124 M^{-1} cm^{-1}),[45] but the ϵ_{max} values are lower in our case. We believe that these differences in ϵ_{max} values are due to different temperatures of measurement. From the magnetic moment measurements in acetonitrile (last column, Table 1), it can be seen that both species [Fe(**1**)$(CH_3CN)_2]^{2+}$ and [Fe(**2**)$(CH_3CN)_2]^{2+}$ are, at room temperature, in a spin crossover regime: μ_{eff}= 0.98μ_B at 298 K for [Fe(**1**)OTf_2] (cf. μ_{eff}= 0.87μ_B at 293 K)[29] and μ_{eff}= 4.26μ_B at 298 K for [Fe(**2**)OTf_2]. Within this crossover regime, small temperature variations will strongly affect the intensity of this MLCT band. We have therefore used a thermostatic UV−vis spectrometer, and the values listed in Table 1 correspond to 298 K. Unfortunately, the temperatures at which the reported values were recorded were not given.

From Figure 2 and the ϵ_{max} values listed in Table 1, it can be seen that the intensities are related to the number of pyridine donors and the spin state of the iron(II) center. The largest intensity is observed for complex [Fe(**1**)$(CH_3CN)_2]^{2+}$, which is predominantly low spin and contains three pyridine donors. Complexes [Fe(**2**)$(CH_3CN)_2]^{2+}$ and [Fe(**3**)$(CH_3CN)_2]^{2+}$ have two pyridine donors, but [Fe(**2**)$(CH_3CN)_2]^{2+}$ is partially low spin, which increases the extinction coefficient. In the case of complex [Fe(**4**)$(CH_3CN)_2]^{2+}$ with only one pyridine donor, the MLCT band appears as a mere shoulder and disappears completely for complex [Fe(**5**)$(CH_3CN)]^{2+}$. As expected, the ligand-based transitions in the UV region of the spectrum also decrease in intensity as fewer pyridine donors are present.

(41) Al-Obaidi, A. H. R.; Jensen, K. B.; McGarvey, J. J.; Toftlund, H.; Jensen, B.; Bell, S. E. J.; Carroll, J. G. *Inorg. Chem.* **1996**, *35*, 5055−5060.
(42) Mialane, P.; Nivorojkine, A.; Pratviel, G.; Azéma, L.; Slany, M.; Godde, F.; Simaan, A. J.; Banse, F.; Kargar-Grisel, T.; Bouchoux, G.; Sainton, J.; Horner, O.; Guilhem, J.; Tchertanova, L.; Meunier, B.; Girerd, J.-J. *Inorg. Chem.* **1999**, *38*, 8.
(43) Toftlund, H.; Yde-Andersen, S. *Acta Chem. Scand.* **1981**, *A35*, 575−585.
(44) Bernal, I.; Jensen, I. M.; Jensen, K. B.; McKenzie, C. J.; Toftlund, H.; Tuchagues, J.-P. *J. Chem. Soc., Dalton Trans.* **1995**, 3667−3675.
(45) White, M. C.; Doyle, A. G.; Jacobsen, E. N. *J. Am. Chem. Soc.* **2001**, *123*, 7194−7195.

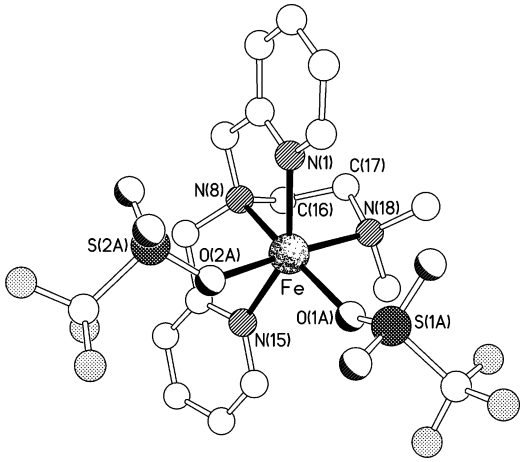

Figure 3. Molecular structure of [Fe(**3**)OTf_2].

Table 2. Selected Bond Lengths (Å) and Angles (deg) for [Fe(**3**)OTf_2]

Fe−O(1A)	2.088(3)	Fe−O(2A)	2.240(4)
Fe−N(1)	2.161(4)	Fe−N(8)	2.238(4)
Fe−N(15)	2.174(4)	Fe−N(18)	2.242(4)
O(1A)−Fe−N(1)	110.13(14)	O(1A)−Fe−N(15)	99.07(14)
N(1)−Fe−N(15)	148.67(15)	O(1A)−Fe−N(8)	168.28(15)
N(1)−Fe−N(8)	77.36(14)	N(15)−Fe−N(8)	75.84(14)
O(1A)−Fe−O(2A)	85.01(14)	N(1)−Fe−O(2A)	87.95(15)
N(15)−Fe−O(2A)	83.40(15)	N(8)−Fe−O(2A)	104.62(15)
O(1A)−Fe−N(18)	88.32(15)	N(1)−Fe−N(18)	91.91(14)
N(15)−Fe−N(18)	100.26(14)	N(8)−Fe−N(18)	82.31(15)
O(2A)−Fe−N(18)	172.84(14)		

Solid-State Structures. Single crystals suitable for X-diffraction of [Fe(**3**)OTf_2] and [Fe(**5**)OTf_2] were obtained from a dichloromethane (DCM)/pentane solution. The X-ray structure of [Fe(**3**)OTf_2] shows it to have a severely distorted octahedral geometry at the iron center, the N(1)−Fe−N(15) angle being 148.67(15)° (Figure 3); this distortion is a consequence of two contiguous restricted bite five-membered N,N′ chelate rings, the N(1)−Fe−N(8) and N(8)−Fe−N(15) angles being 77.36(14)° and 75.84(14)°, respectively (Table 2). By contrast, the O(1A)−Fe−N(8) and O(2A)−Fe−N(18) trans angles are 168.28(15)° and 172.84(14)°, respectively. This geometry is similar to that seen in the closely related structure [Fe(**1**)OTf_2] where the N(pyridyl)−Fe−N(pyridyl) trans angle is 153.46(8)° and the two associated N,N′ chelate bite angles are 78.26(8)° and 75.79(8)°.[29] Here in [Fe(**3**)OTf_2], the two N(1)/N(8) and N(8)/N(15) five-membered chelate rings both have envelope geometries with N(8) lying ca. 0.22 and ca. 0.29 Å out of the {C_2N(1),Fe} and {C_2N(15),Fe} planes, respectively, (the former being coplanar to within ca. 0.03 Å, and the latter coplanar to better than 0.01 Å). The N(8)/N(18) five-membered chelate ring adopts a twisted conformation with C(16) lying ca. 0.42 Å "below" the {N(8),N(18),Fe} plane and C(17) lying ca. 0.29 Å "above" it giving, in the picture as drawn, a δ-twist to the ring. (The complex has crystallized in a racemic space group so half of the molecules in the crystal will have a λ-twist for this ring.) The Fe−N distances reflect the different chemical nature of the donor atoms with those to the pyridyl nitrogens N(1) and N(15) [2.161(4) and 2.174(4) Å, respectively] being noticeably shorter than those to the amine nitrogens N(8) and N(18) [2.238(4) and 2.242(4) Å, respectively], though they are all typical of high-spin Fe(II)

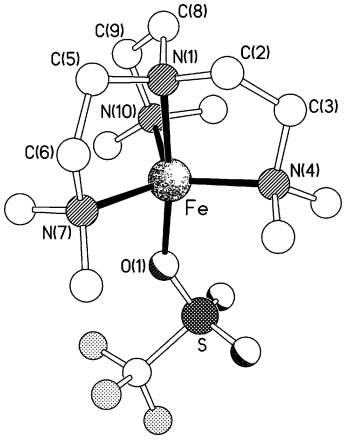

Figure 4. Molecular structure of the cation in [Fe(**5**)OTf]OTf.

complexes.[18,46,47] The two Fe−O distances are very different from each other with that to O(1A) [2.088(3) Å] being markedly shorter than that to O(2A) [2.240(4) Å]. The lengths for the comparable bonds in [Fe(**1**)OTf_2] are 2.054(2) and 2.150(2) Å.[29] For complex [Fe(**1**)OTf_2], this difference can simply be explained by considering the amine/pyridyl nature of the trans donor atoms; the two Fe−N distances are 2.203(2) and 2.179(2) Å, respectively, with the longer Fe−O bond being trans to the shorter Fe−N bond, and vice versa. Here in [Fe(**3**)OTf_2], however, the Fe−O bonds are both trans to amine donors for which the Fe−N bond lengths are identical (vide supra). This suggests that the difference in the Fe−O distances might be due to steric effects rather than an electronic trans influence. Alternatively, it could also be viewed as an increased preference of this complex to attain a five-coordinate geometry. Crystal packing forces can be excluded as a major factor as there are no noteworthy intermolecular interactions.

The solid-state structure of [Fe(**5**)OTf]OTf shows a five-coordinate trigonal bipyramidal geometry at the iron center (Figure 4), similar to that seen in the structure of [Fe(**5**)Br]-Br.[31,32] Though [Fe(**5**)OTf]OTf cannot have the crystallographic C_3 symmetry seen in the bromo analogue, the tetradentate ligand does adopt a conformation with approximate molecular C_3 symmetry (see Figure S3 in the Supporting Information). The axial···equatorial cis angles involving N(1) are all noticeably smaller [between 82.90(19)° and 83.3(2)°] than their O(1) counterparts [92.5(2)−103.6(2)°], reflecting the displacement of the iron atom "below" the equatorial N_3 plane toward O(1) by ca. 0.26 Å. (This deviation was ca. 0.32 Å in the bromo species.) The equatorial···equatorial cis angles range between 116.2(2)° and 120.4(2)° (cf. 117.8(5)° in [Fe(**5**)Br]Br), while the axial···axial trans angle is 173.1(2)° (Table 3). The three five-membered N,N′ chelate rings all have twisted conformations; C(2) and C(3) lie ca. +0.27 and −0.37 Å, respectively, out of the {N(1),N(4),Fe} plane, C(5) and C(6) lie ca. +0.33 and −0.29 Å, respectively, out of the {N(1),N(7),Fe} plane, and C(8) and C(9) lie ca. +0.26 and −0.40 Å, respectively, out of the {N(1),N(10),Fe} plane, giving each ring (as drawn in Figures 3 and S3) a λ-twist. (As with [Fe(**3**)OTf_2], the complex has crystallized in a racemic space group so 50% of the molecules in the crystal will have the opposite (δ) twist for these rings.) The estimated standard deviations for the bond lengths and angles in [Fe(**5**)Br]Br are sufficiently large that meaningful comparisons with the OTf species cannot be made, but it is noticeable that the Fe−N(amine) bond lengths here in [Fe(**5**)OTf]OTf [which range between 2.156(5) and 2.177(5) Å] are noticeably shorter than their counterparts in [Fe(**3**)OTf_2], probably a consequence of both the cationic nature of [Fe(**5**)OTf]OTf and its lower coordination number. The same can be said for the Fe−O bond length which, at 2.043(4) Å, is ca. 0.04 Å shorter than the shortest of the two in [Fe(**3**)OTf_2] (vide supra). There are no intermolecular interactions of note.

Table 3. Selected Bond Lengths (Å) and Angles (deg) for [Fe(**5**)OTf]OTf

Fe−O(1)	2.043(4)	Fe−N(1)	2.177(5)
Fe−N(4)	2.156(5)	Fe−N(7)	2.166(5)
Fe−N(10)	2.171(5)		
O(1)−Fe−N(4)	103.6(2)	O(1)−Fe−N(7)	92.5(2)
N(4)−Fe−N(7)	116.2(2)	O(1)−Fe−N(10)	94.6(2)
N(4)−Fe−N(10)	119.1(2)	N(7)−Fe−N(10)	120.4(2)
O(1)−Fe−N(1)	173.1(2)	N(4)−Fe−N(1)	83.2(2)
N(7)−Fe−N(1)	83.3(2)	N(10)−Fe−N(1)	82.90(19)

We can conclude from the solution and solid-state studies on the series of iron(II) bis(triflate) complexes containing ligands **1**−**5** that, in DCM solution and in the solid state, all complexes are high spin at room temperature and their preferred geometry changes from six-coordinate for ligands **1**−**3** to five-coordinate for ligand **5**, whereby in the case of ligand **4**, an intermediate behavior is observed. In acetonitrile solution, the triflate ligands are largely displaced by acetonitrile ligands, causing a low-spin configuration at room temperature in the case of ligand **1** and at −40 °C for ligand **2**. This is due to the stronger ligand field exerted by the acetonitrile ligands, which, in the order from **1** to **5**, is counteracted by the weaker ligand field exerted by dimethylamino donors, resulting in high-spin configurations in the case of ligands **3**−**5**. These observations may prove important in understanding the catalytic properties of these complexes in oxidation catalysis.

Catalytic Oxidation of Cyclohexane. The catalytic properties of the iron(II) bis(triflate) complexes containing ligands **1**−**5** for the oxidation of cyclohexane with H_2O_2 have been evaluated (eq 3).

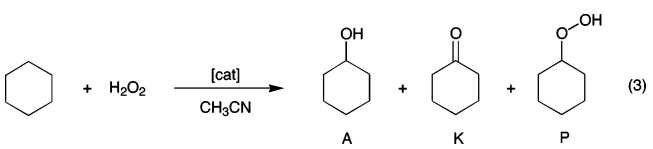

The oxidation reactions were carried out in acetonitrile as the solvent at room temperature under air. Hydrogen peroxide solution (70 mM, 10 equiv) was added to an acetonitrile solution containing the catalyst (2.1 μmol, 1 equiv) and cyclohexane (2.1 mmol, 1000 equiv). A large excess of substrate was used to minimize over-oxidation of cyclohex-

(46) Simaan, J.; Poussereau, S.; Blondin, G.; Girerd, J.-J.; Defaye, D.; Philouze, C.; Guilhem, J.; Tchertanov, L. *Inorg. Chim. Acta* **2000**, *299*, 221−230.
(47) Gütlich, P.; Garcia, Y.; Goodwin, H. A. *Chem. Soc. Rev.* **2000**, *29*, 419−427.

Table 4. Catalytic Results of the Oxidation of Cyclohexane with H_2O_2[a]

run	catalyst	H_2O_2 equiv	yield A + K[b] %	A/K[c]	P[d]	KIE	adamantane 3°/2°
1	$FeOTf_2(CH_3CN)_2$	10	4	1.6	Y	nd	7
2	$FeOTf_2(CH_3CN)_2$	100	3	2.4	Y	1.7	
3	Fe(**1**)OTf_2 (tpa)	10	32	12.0	N	3.5	18
4	Fe(**1**)OTf_2	100	29	5.9	N	3.1	
5	Fe(**2**)OTf_2 (bpmen)	10	65	9.5	N	2.9	13
6	Fe(**2**)OTf_2	100	48	2.5	N	2.4	
7	Fe(**3**)OTf_2 (*iso*-bpmen)	10	32	6.8	N	3.4	23
8	Fe(**3**)OTf_2	100	6.6	4.4	Y	2.9	
9	Fe(**4**)OTf_2 (Me_4-benpa)	10	3.4	3.7	Y	2.1	7
10	Fe(**4**)OTf_2	100	1.3	1.6	Y	2.0	
11	Fe(**5**)OTf_2 (Me_6-tren)	10	3.2	1.3	Y	1.8	6
12	Fe(**5**)OTf_2	100	1.0	1.2	Y	1.8	

[a] Conditions: see Experimental Section. [b] Total percentage yield of cyclohexanol (A) + cyclohexanone (K), expressed in moles of product per mole of H_2O_2. [c] Ratio of cyclohexanol (A) to cyclohexanone (K). [d] Qualitative analysis of cyclohexyl hydroperoxide (P), Y: observed in GC, N: not observed in GC.

anol (A) to cyclohexanone (K). The addition of dilute H_2O_2 was carried out slowly using a syringe pump to minimize H_2O_2 decomposition. The yields are based on the amount of oxidant (H_2O_2) converted into oxygenated products. Two series of catalytic experiments were carried out initially, using 10 and 100 equiv of H_2O_2. The results are summarized in Table 4.

The yield of total oxidation products (A + K) varies substantially for the different catalysts. The most active catalyst [Fe(**2**)OTf_2] converts 65% of the H_2O_2 added into oxygenated products, with a large A/K ratio. The TPA complex [Fe(**1**)OTf_2] gives a conversion of 32% but with a better A/K ratio. These results are comparable to those reported by Que and co-workers when using the complexes [Fe(**1**)$(CH_3CN)_2$]$(ClO_4)_2$ and [Fe(**2**)$(CH_3CN)_2$]$(ClO_4)_2$ as catalysts, and we have used these results as benchmarks with which to compare our catalysts.[18] Complex [Fe(**3**)OTf_2] gives a similar conversion as [Fe(**1**)OTf_2], but the A/K ratio is significantly reduced. Complexes [Fe(**4**)OTf_2] and [Fe(**5**)-OTf_2] give only very low conversions, similar to the amounts obtained with $FeOTf_2(CH_3CN)_2$. These low conversions, combined with the low A/K ratios, are indicative of Fenton-type chemistry, which involves a radical chain auto-oxidation mechanism. This is also supported by the observation of cyclohexyl hydroperoxide (P) in these cases.[22]

A larger hydrogen peroxide concentration (700 mM, 100 equiv) results, in the case of the complexes containing ligands **1**−**2**, in a lower percentage yield (i.e., a lower percentage conversion of H_2O_2 into oxygenated products) and in a reduction of the A/K ratio. This lower relative yield at higher H_2O_2 concentration is most likely due to an increase in nonproductive processes such as the decomposition of H_2O_2 and the over-oxidation of cyclohexanol to cyclohexanone. Complex [Fe(**3**)OTf_2] gives a much lower yield, and the presence of cyclohexyl hydroperoxide indicates the presence of Fenton-type chemistry in this case.

The kinetic isotope effect values (KIE, see Table 4) for the oxidation of cyclohexane using the various catalysts have been determined from competition experiments using a mixture of cyclohexane and perdeuterated cyclohexane. In the case of a Fenton-type radical auto-oxidation mechanism, the KIE is expected to be close to 1, whereas in the case of a metal-based oxidation, a higher value is expected, up to the classical maximum of about 7 for the primary KIE. It can be seen that, for the catalysts containing ligands **1**−**3**, the KIE values range from 2.9 to 3.5 at the lower H_2O_2 concentration, whereas the other systems containing **4** and **5** (and also $FeOTf_2(CH_3CN)_2$) give values around 2 or lower. These values, which are comparable to values reported previously by Que for complexes [Fe(**1**)$(CH_3CN)_2$]$(ClO_4)_2$ and [Fe(**2**)$(CH_3CN)_2$]$(ClO_4)_2$,[18] indicate that, in the catalyst systems containing ligands **1**−**3,** a more selective metal-based oxidant is operating rather than the unselective OH radicals.

Another method that has been previously used to probe the nature of the oxidant is the oxidation of adamantane, which contains both secondary (2°) and tertiary (3°) C−H bonds.[11] The indiscriminate OH radicals typically afford values for 3°/2° around 2, whereas more selective oxidants give substantially higher values. From the last column in Table 4, it can be seen that the catalyst systems containing ligands **1**−**3** appear to be much better in discriminating between the oxidation of tertiary versus secondary C−H bonds compared to the other catalyst systems. Thus far, we can conclude that the catalyst systems [Fe(**1**)OTf_2], [Fe(**2**)-OTf_2], and [Fe(**3**)OTf_2] (at least at lower H_2O_2 concentration) appear to be more active and selective catalysts than [Fe-(**4**)OTf_2] and [Fe(**5**)OTf]OTf.

To obtain a better understanding of the catalytic properties of the more active complexes containing ligands **1**−**3** and the differences between these catalysts, we have monitored the product distribution with increasing amounts of oxidant. Samples were taken after the addition of various amounts of H_2O_2, ranging from 2 to 50 equiv, while keeping the speed of addition constant at 0.72 mL/h (24 equiv/h). The amount of cyclohexanol (A) and cyclohexanone (K), as well as the total amount (A + K), has been plotted against the amount of H_2O_2 added (see Figure 5). All data points have been duplicated and fitted to a 2nd order polynomial trend line. The diagonal (dotted line) represents the theoretical maximum amount of oxidation products that can be obtained if all H_2O_2 were converted into oxidized hydrocarbon products.

The results presented here follow on from a study carried out previously by Que and co-workers on the catalyst [Fe-(**1**)$(CH_3CN)_2$]$(ClO_4)_2$, where it was found that with up to 10 equiv of H_2O_2, the amounts of A and K increased linearly,

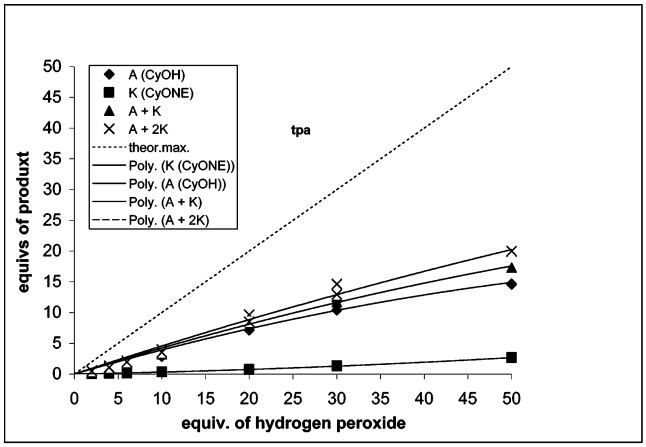

a) [Fe(**1**)OTf$_2$] (tpa)

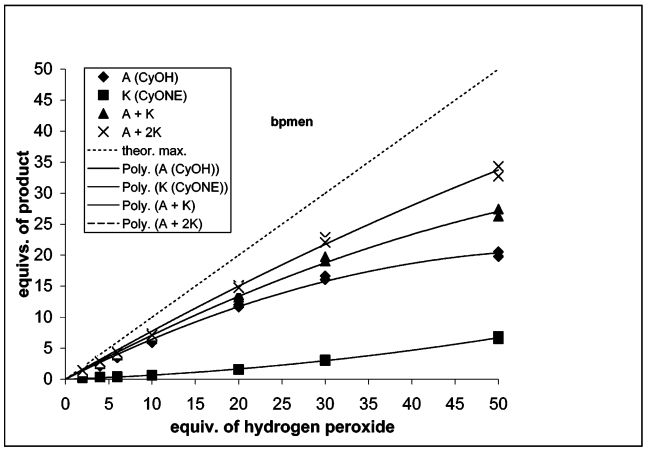

b) [Fe(**2**)OTf$_2$] (bpmen)

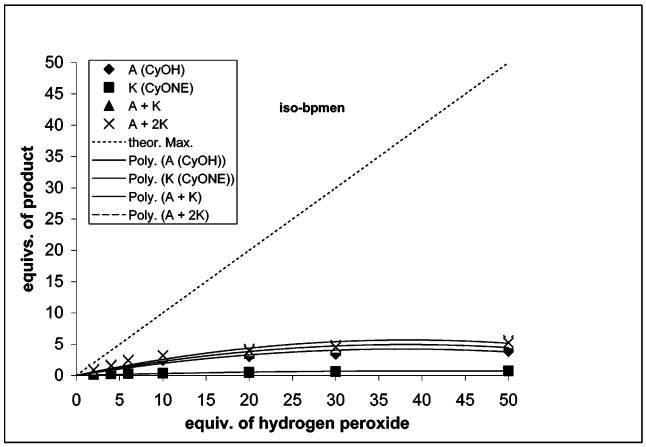

c) [Fe(**3**)OTf$_2$] (*iso*-bpmen)

Figure 5. Product composition of cyclohexane oxidation at different amounts of H_2O_2 added.

whereas upon addition of more equivalents, some deviation from linearity becomes apparent.[18] From the graph in Figure 5a, it can be seen that, for the catalyst [Fe(**1**)OTf$_2$], the addition of more H_2O_2 up to 50 equiv results in more cyclohexanol (A), but this is not the only oxidation product and it does not follow the diagonal. This deviation may be due to several reasons, including (1) over-oxidation of cyclohexanol to cyclohexanone, (2) decomposition of H_2O_2, and (3) catalyst decomposition. The formation of cyclohexanone due to over-oxidation is clearly evident and becomes more pronounced when more H_2O_2 is added, i.e., when more alcohol is present relative to alkane. We have shown in separate experiments that cyclohexanol is oxidized to cyclohexanone under these conditions. However, if this were the only side reaction and all the H_2O_2 added was used to oxidize cyclohexane and cyclohexanol only, the number of equivalents of A + 2K versus equivalents of H_2O_2 added should be linear and coincide with the diagonal. For all catalysts, the A + 2K curves show a significant deviation from the diagonal, which we believe is mainly due to the decomposition of H_2O_2. By generating a powerful oxidation catalyst that can oxidize alkanes, the oxidation of H_2O_2 to H_2O and O_2 is likely to become more pronounced. The loss of oxidant appears to be less for [Fe(**1**)OTf$_2$] and [Fe(**2**)OTf$_2$], compared to [Fe(**3**)OTf$_2$]. Finally, the A + 2K curves also show a deviation from linearity, which we believe is due to catalyst deactivation. The bpmen catalyst [Fe(**2**)OTf$_2$] appears to be the most robust catalyst, followed by [Fe(**1**)OTf$_2$], whereas the *iso*-bpmen derivative [Fe(**3**)OTf$_2$] has a much shorter lifetime.

In conclusion, we have shown for the series of iron(II) bis(triflate) complexes containing tetradentate nitrogen ligands that, in the order from **1** to **5**, the preferred coordination geometry of the complexes changes from six-coordinate to five-coordinate. In acetonitrile solution, the triflate ligands are largely uncoordinated and acetonitrile complexes are formed. More pyridine donors results in increased charge transfer from the metal to the ligand, as shown by an increase in intensity of the characteristic MLCT band around 400 nm in the UV−vis spectrum. All complexes catalyze the oxidation of cyclohexane with H_2O_2, but only the complexes containing ligands **1**−**3** with at least two pyridine donors show a reactivity that is distinct from Fenton-type chemistry. It therefore appears that pyridine donors are essential for high catalytic activity and selectivity in these systems, which may be related to the increased charge transfer from the metal to the ligand, i.e., a stronger ligand field, which stabilizes the intermediates responsible for metal-based oxidation. The two complexes of the ligands **4** and **5**, containing more amine than pyridine donors, appear to be less stable and degrade quickly under the reaction conditions, probably to form oxo-bridged iron(III) species. In addition, these complexes prefer five-coordinate geometries, thereby lacking the availability of two cis coordination sites at the metal center, which is thought to be important for catalytic activity. Several issues remain, such as the decomposition of H_2O_2 and the catalyst, and we are therefore continuing our quest for a catalyst system that converts all oxidant into product, with maximum activity and selectivity and an acceptable catalyst lifetime.

Experimental Section

General. All moisture-sensitive compounds were manipulated using standard vacuum line, Schlenk, or cannula techniques or in a conventional nitrogen-filled glovebox. NMR spectra were recorded either on a Bruker AC-250 or a DRX-400 spectrometer; chemical shifts for ^{1}H and ^{13}C NMR are referenced to the residual protio impurity and to the ^{13}C NMR signal of the deuterated solvent, whereas ^{19}F NMR is referenced to $CFCl_3$. Mass spectra were

recorded on either a VG Autospec or a VG Platform II spectrometer. Elemental analyses were performed by the Science Technical Support Unit at the London Metropolitan University. GC analysis was carried out on an Agilent 6890A gas chromatograph with a HP-5 column (30 m × 0.32 mm, film thickness 0.25 μm) or an Innowax column (30 m × 0.25 mm, film thickness 0.25 μm). Toluene was used as the standard for quantitative analysis. Magnetic moments were determined by the Evans' NMR method.[48] UV−vis spectra were recorded at 25 °C in acetonitrile solution on a Perkin-Elmer Lambda 2 spectrometer.

Solvents and Reagents. Toluene and pentane were dried by passing through a column, filled with commercially available Q-5 reagent (13 wt% CuO on alumina) and activated alumina (pellets, 3 mm). Diethyl ether and tetrahydrofuran were dried over potassium metal with a benzophenone ketyl indicator, whereas DCM and acetonitrile were dried over CaH_2. The synthesis of the metal precursor $Fe(OTf)_2(CH_3CN)_2$,[49,50] and the complexes [Fe(**1**)OTf_2],[29] [Fe(**1**)$(CH_3CN)_2$][ClO_4]$_2$,[39] and [Fe(**5**)Br]Br[31,32] have been reported previously. Bis(*N*,*N*-dimethylaminoethyl)amine[51] was prepared according to a published procedure. All other chemicals and NMR solvents were obtained commercially and used as received.

Tris(2-pyridylmethyl)amine (tpa) (1). To a mixture of 0.54 g (5.26 mmol) of 2-(aminomethyl)pyridine and 3.12 g (14.7 mmol) of sodium triacetoxyborohydride stirring in DCM (75 mL) was added 1.00 mL (10.5 mmol) of pyridine-2-carboxaldehyde. Upon completion of addition, stirring was continued for a further 18 h. Subsequently, a saturated aqueous sodium hydrogen carbonate solution was added, and after 15 min of stirring, an extraction of the mixture using ethyl acetate was performed. The organic fraction was dried ($MgSO_4$), and the solvent removed. The residue was extracted several times with small quantities of petroleum ether (40−60 °C); the extracts were combined and the solvent removed to give **1** as a yellow solid (1.10 g, 72%). ^{1}H NMR ($CDCl_3$): δ 8.53 (d, 3H, 6-Py*H*), 7.63 (m, 6H, 3-Py*H* and 4-Py*H*), 7.14 (t, 3H, 5-Py*H*), 3.88 (s, 6H, NCH_2).^{13}C NMR ($CDCl_3$): δ 159.3 (*ipso*), 149.1, 136.4, 123.0, 122.0, 60.1 (NCH_2). MS (+EI): *m*/*z* (%) 290 (2) [M^+], 212 (1) [$(M - Py)^+$], 198 (100) [$(M - PyCH_2)^+$], 171 (11), 119 (10) [$(PyCH_2NCH)^+$], 93 (48) [$(PyMe)^+$].

***N*,*N*′-Bis(2-pyridylmethyl)-*N*,*N*′-dimethylethane-1,2-diamine (bpmen) (2).** To a solution of *N*,*N*′-dimethylethane-1,2-diamine (0.71 mL, 6.62 mmol) and 2 equiv of pyridine-2-carboxaldehyde (1.26 mL, 13.2 mmol), in DCM (100 mL), was added 2.8 equiv of sodium triacetoxyborohydride (3.93 g, 18.5 mmol). The mixture obtained was stirred for 12 h. Afterward, saturated aqueous sodium hydrogen carbonate solution was added, and stirring continued for a further 15 min prior to extraction with ethyl acetate. The organic layer was dried over magnesium sulfate, filtered, and reduced to dryness. The oily residue was dissolved in THF (50 mL) and treated with KH (0.18 g, 4.41 mmol) to remove traces of pyridine carbinol. After the mixture was stirred for 90 min, the solvent was removed and the residue was extracted with several portions of pentane. The pentane extracts were combined and all volatiles removed to give **2** as a pale yellow oil (1.05 g, 59%). ^{1}H NMR ($CDCl_3$): δ 8.48 (d, 2H, 6-Py*H*), 7.56 (t, 2H, 4-Py*H*), 7.36 (d, 2H, 3-Py*H*), 7.10 (t, 2H, 5-Py*H*), 3.63 (s, 4H, PyCH_2), 2.60 (s, 4H, NCH_2CH_2N), 2.22 (s, 6H, N*Me*). ^{13}C NMR ($CDCl_3$): δ 158.9 (*ipso*), 148.6, 136.1, 122.8, 121.6, 63.8 (PyCH_2), 55.1 (NCH_2CH_2N), 42.5 (N*Me*). MS (+EI): *m*/*z* (%) 270 (4) [M^+], 178 (2) [$(M - PyCH_2)^+$], 135 (100) [$(PyCH_2N(Me)CH_2)^+$], 92 (42) [$(PyCH_2)^+$].

***N*,*N*-Bis(2-pyridylmethyl)-*N*′,*N*′-dimethylethane-1,2-diamine (*iso*-bpmen) (3).** To a stirring mixture of 0.50 mL (4.54 mmol) of *N*,*N*-dimethylethane-1,2-diamine and 3.75 g (17.7 mmol) of sodium triacetoxyborohydride in DCM (100 mL) was added 1.30 mL (13.6 mmol) of pyridine-2-carboxaldehyde, after which stirring was continued for a further 18 h. The reaction was quenched with saturated aqueous sodium hydrogen carbonate and extracted using ethyl acetate (3 × 150 mL). The organic fractions were combined, dried ($MgSO_4$), and the solvent removed using a rotary evaporator. The residue was dissolved in THF (50 mL) and treated with KH (0.36 g, 9.08 mmol). After the mixture was stirred for 2 h, the solvent was removed and the residue was extracted with copious quantities of pentane. The pentane extracts were reduced to dryness to give **3** as a pale yellow oil (1.13 g, 92%). ^{1}H NMR ($CDCl_3$): δ 8.44 (d, 2H, 6-Py*H*), 7.57 (t, 2H, 4-Py*H*), 7.45 (d, 2H, 3-Py*H*), 7.06 (t, 2H, 5-Py*H*), 3.77 (s, 4H, $PyCH_2$), 2.62 (m, 2H, NCH_2CH_2-NMe_2), 2.42 (m, 2H, $NCH_2CH_2NMe_2$), 2.09 (s, 6H, N*Me*). ^{13}C NMR ($CDCl_3$): δ 159.6 (*ipso*), 148.9, 136.3, 123.0, 121.9, 60.7 (PyCH_2), 57.2 ($PyCH_2NCH_2$), 52.2 (CH_2NMe_2), 45.6 (N*Me*). MS (+EI): *m*/*z* (%) 270 (5) [M^+], 212 (100) [$(M - CH_2NMe_2)^+$], 200 (7) [$(M - C_2H_2NMe_2)^+$], 178 (12) [$(M - PyCH_2)^+$], 119 (44) [$(PyCH_2NCH)^+$].

Bis[2-(dimethylamino)ethyl](2-pyridylmethyl)amine (Me_4-benpa) (4). Pyridine-2-carboxaldehyde (0.59 mL, 6.16 mmol) was added to a mixture of 0.98 g (6.15 mmol) of bis[2-(dimethylamino)-ethyl]amine and 1.83 g (8.61 mmol) of sodium triacetoxyborohydride in DCM (50 mL) and allowed to stir for 12 h. The reaction was quenched with 3 M aqueous sodium hydroxide and extracted using copious amounts of DCM. The DCM fractions were combined, dried ($MgSO_4$), and the solvent removed using a rotary evaporator. The residue obtained was dissolved in THF (50 mL) and treated with KH (0.25 g, 6.15 mmol). After being stirred for 2 h, the solvent was removed and the residue was extracted with pentane. The pentane extracts were combined and all volatiles removed to give **4** as a pale yellow oil (1.30 g, 85%). ^{1}H NMR ($CDCl_3$): δ 8.47 (d, 1H, 6-Py*H*), 7.59 (t, 1H, 4-Py*H*), 7.43 (d, 1H, 3-Py*H*), 7.09 (t, 1H, 5-Py*H*), 3.75 (s, 2H, PyCH_2), 2.62 (m, 4H, N$CH_2CH_2NMe_2$), 2.38 (m, 4H, $NCH_2CH_2NMe_2$), 2.15 (s, 12H, N*Me*). ^{13}C NMR ($CDCl_3$): δ 160.1 (*ipso*), 148.9, 136.3, 122.9, 121.8, 61.3 (PyCH_2), 57.5 ($PyCH_2NCH_2$), 52.8 (CH_2NMe_2), 45.9 (N*Me*). MS (+EI): *m*/*z* (%) 250 (25) [M^+], 192 (39) [$(M - CH_2$-$NMe_2)^+$], 149 (20) [$(M - (CH_2NMe_2)(CH_2NMe))^+$], 93 (17) [$(PyMe)^+$], 72 (100) [$(CH_2N(Me)(Et))^+$], 58 (56) [$(CH_2NHEt)^+$].

Tris[2-(dimethylamino)ethyl]amine (Me_6-TREN) (5). Aqueous formaldehyde (49.0 mL, 660 mmol, 37 wt%) was added to a solution of 3.00 mL (19.9 mmol) of tren and 135 mL of acetic acid in acetonitrile (600 mL) and allowed to stir for 1 h. Subsequently, the reaction mixture was cooled to 0 °C and 10.0 g (13.4 mmol) of sodium borohydride slowly added. After being stirred for 48 h, all solvents were removed, the residue was made strongly basic with 3 M aqueous sodium hydroxide, and extracted several times with DCM. The DCM extracts were combined, dried ($MgSO_4$), and the solvent removed. The residue was dissolved in pentane, filtered, and the filtrate reduced to dryness to give **5** as pale yellow oil (4.32 g, 94%). ^{1}H NMR ($CDCl_3$): δ 2.55 (m, 6H, CH_2NMe_2), 2.32 (m, 6H, N$CH_2CH_2NMe_2$), 2.16 (s, 18H, N*Me*).

***N*,*N*′-Dimethyl-*N*,*N*′-bis(2-pyridylmethyl)ethane-1,2-diamine Iron(II) Bis(triflate) [Fe(2)OTf_2].** Stirring a mixture of **2** (0.15 g, 0.55 mmol) and $Fe(OTf)_2(CH_3CN)_2$ (0.24 g, 0.55 mmol) in THF overnight gave a yellow precipitate. The volume of solvent

(48) Britovsek, G. J. P.; Gibson, V. C.; Spitzmesser, S. K.; Tellmann, K. P.; White, A. J. P.; Williams, D. J. *J. Chem. Soc., Dalton Trans.* **2002**, 1159−1171.
(49) Bryan, P. S.; Dabrowiak, J. C. *Inorg. Chem.* **1975**, *14*, 296−299.
(50) Hagen, K. S. *Inorg. Chem.* **2000**, *39*, 5867−5869.
(51) Luitjes, H.; Schakel, M.; Klumpp, G. W. *Synth. Commun.* **1994**, *24*, 2257.

was reduced to about 10 mL, and the mixture filtered. The solid was washed twice with small volumes of THF and dried under vacuum to give a yellow powder (0.22 g, 64%). ^{1}H NMR (CD_2Cl_2): δ 169.4 (2H, Py*H*α), 123.5 (2H, C*H*$_2$Py), 94.4 (2H, C*H*$_2$Py), 74.7 (6H, N*Me*), 54.8 (2H, Py*Hβ*), 53.6 (2H, Py*Hβ′*), 28.4 (2H, NC*H*$_2$), 15.9 (2H, NC*H*$_2$), −15.6 (2H, Py*Hγ*).^{1}H NMR (CD_3CN): δ 81.2 (2H, Py*H*α), 64.1 (2H, C*H*$_2$Py), 41.8 (6H, N*Me*), 27.2 (8H, NC*H*$_2$, C*H*$_2$Py and Py*Hβ*), 13.8 (2H, Py*Hβ*), 0.6 (2H, Py*Hγ*).^{19}F NMR (CD_2Cl_2): δ −29.1.^{19}F NMR (CD_3CN): δ −77.3. MS (+FAB): *m*/*z* (%) 624 [M$^+$], 475 [(M − OTf)$^+$]. Anal. Calcd (found) for $C_{26}H_{22}Cl_2FeN_4$: C, 34.63 (34.78); H, 3.55 (3.65); N, 8.97 (8.77). μ_{eff} (CD_2Cl_2) = 5.27μ_B. μ_{eff} (CD_3CN) = 4.26μ_B.

***N*,*N*-Dimethyl-*N*′,*N*′-bis(2-pyridylmethyl)ethane-1,2-diamine Iron(II) Bis(triflate) [Fe(3)OTf$_2$].** A solution of Fe(OTf)$_2$(CH_3CN)$_2$ (1.06 g, 2.43 mmol) in THF (30 mL) was added to a solution of **3** (0.73 g, 2.70 mmol) in THF (30 mL), and the resultant mixture was stirred overnight. The volume of solution was reduced to approximately 10 mL, and pentane was added to precipitate solid, which was isolated by filtration and washed twice with small quantities of DCM. The yellow powder obtained was recrystallized by slow diffusion from a DCM solution layered with pentane to give the product as yellow crystals (1.06 g, 70%), which were suitable for X-ray analysis. ^{1}H NMR (CD_2Cl_2): δ 144.8 (2H, Py*H*α), 120.5 (2H, C*H*$_2$), 104.5 (6H, N*Me*), 48.0 (4H, Py*Hβ*), 47.6 (2H, Py*Hβ′*), 18.9 (2H, Py*Hγ*). 3.1 (2H, C*H*$_2$). ^{1}H NMR (CD_3CN): δ 112.0 (2H, Py*H*α), 99.9 (6H, N*Me*), 50.9 (2H, Py*Hβ*), 45.8 (3H, Py*Hβ′*), 41.3 (1H, C*H*$_2$), 8.9 (2H, C*H*$_2$), −1.8 (2H, Py*Hγ*).^{19}F NMR (CD_2Cl_2): δ −23.7.^{19}F NMR (CD_3CN): δ −66.2. MS (+FAB): *m*/*z* 1099 [(2M − OTf)$^+$], 624 [M$^+$], 475 [(M − OTf)$^+$]. Anal. Calcd (found) for $C_{18}H_{22}F_6FeN_4O_6S_2$: C, 34.63 (34.59); H, 3.55 (3.53); N, 8.97 (8.85). μ_{eff} (CD_2Cl_2) = 5.32μ_B. μ_{eff} (CD_3CN) = 4.72μ_B.

Bis(2-dimethylaminoethyl)(2-pyridylmethyl)amine Iron(II) Dibromide [Fe(4)Br$_2$]. Me$_4$-benpa (**4**, 0.92 g, 3.67 mmol) dissolved in *n*-butanol (5 mL) was added to a hot solution of $FeBr_2$ (0.66 g, 3.06 mmol), in *n*-butanol (10 mL), and the resultant mixture stirred for 10 min under reflux. Upon cooling, the dark solution was reduced to dryness. Trituration of the residue with pentane gave a beige solid, which was isolated by filtration and dried under vacuum. Recrystallization by slow diffusion of a DCM solution of the solid layered with pentane gave a mixture of yellow solid and darkly colored impurities. Addition of acetone to the solid led only to the dissolution of the yellow material. The acetone solution was separated, reduced in volume to approximately 10 mL, and pentane added to precipitate the product. Filtration and drying of the solid under vacuum gave the product as a yellow powder (1.05 g, 74%). ^{1}H NMR (CD_2Cl_2): δ 158.0 (12H, N*Me*), 110.4 (1H, Py*H*α), 107.5 (1H, C*H*$_2$), 81.3 (1H, C*H*$_2$), 65.9 (2H, C*H*$_2$), 59.7 (1H, Py*Hβ*), 57.4 (2H, C*H*$_2$), 55.4 (1H, Py*Hβ′*), −16.0 (1H, Py*Hγ*). MS (+ FAB): *m*/*z* 385 ([M − Br]$^+$), 251 ([M − $FeBr_2$]$^+$). Anal. Calcd (found) for $C_{14}H_{26}Br_2FeN_4$: C, 36.08 (35.84); H, 5.62 (5.62); N, 12.02 (11.93). μ_{eff} (CD_2Cl_2) = 5.23μ_B.

Bis(2-dimethylaminoethyl)(2-pyridylmethyl)amine Iron(II) Bis(triflate) [Fe(4)OTf$_2$]. A mixture of [Fe(**4**)Br$_2$] (0.75 g, 1.61 mmol) and 2 equiv of silver(I) triflate (0.83 g, 3.22 mmol) were stirred in DCM (100 mL) overnight. The mixture was then filtered through Celite, and the filtrate reduced to dryness. The residue obtained was triturated sequentially with pentane and diethyl ether to give a solid that was dried under vacuum. Recrystallization, by slow diffusion of a DCM solution of the solid layered with pentane, gave a crystalline solid and an oily residue. Isolation of the crystals and addition of acetone to them gave a yellow solution and some dark solid impurities. The solution was separated and reduced to dryness. The solid obtained was washed with diethyl ether and dried under vacuum to give the product as a coffee-colored powder (0.74 g, 76%). ^{1}H NMR (CD_2Cl_2): δ 177.2 (6H, N*Me*), 172.4 (6H, N*Me*), 115.1 (2H, C*H*$_2$), 114.0 (1H, Py*H*α), 91.9 (1H, C*H*$_2$), 70.5 (1H, C*H*$_2$), 60.9 (1H, C*H*$_2$), 57.7 (1H, Py*Hβ*), 51.5 (1H, Py*Hβ′*), 49.0 (1H, C*H*$_2$), −17.1 (1H, Py*Hγ*).^{1}H NMR (CD_3CN): δ 139.5 (12H, N*Me*), 115.5 (1H, Py*H*α), 97.8 (1H, C*H*$_2$), 72.1 (1H, C*H*$_2$), 65.7 (1H, Py*Hβ*), 63.0 (1H, C*H*$_2$), 59.1 (1H, C*H*$_2$), 52.8 (1H, Py*Hβ′*), 42.9 (1H, C*H*$_2$), −12.8 (1H, Py*Hγ*). ^{19}F NMR (CD_2Cl_2): δ −43.8. ^{19}F NMR (CD_3CN): δ −68.9. MS (+FAB): *m*/*z* 1059 ([2M − OTf]$^+$), 455 ([M − OTf]$^+$), 251 ([M − Fe(OTf)$_2$]$^+$). Anal. Calcd (found) for $C_{16}H_{26}F_6FeN_4O_6S_2$: C, 31.80 (31.73); H, 4.34 (4.33); N, 9.27 (9.05). μ_{eff} (CD_2Cl_2) = 4.89μ_B. μ_{eff} (CD_3CN) = 4.89μ_B.

Tris(2-dimethylaminoethyl)amine Iron(II) Bis(triflate) [Fe(5)OTf]OTf. A mixture of [Fe(**5**)Br]Br (0.50 g, 1.12 mmol) and 2 equiv of silver(I) triflate (0.58 g, 2.24 mmol) was stirred in DCM (50 mL) overnight. It was subsequently filtered through Celite, and the Celite washed with DCM. The combined filtrate and washings were reduced in volume to approximately 5 mL and pentane added to precipitate the product. The solid was washed with pentane and dried under vacuum to give the product as a white powder (0.52 g, 79%). Crystals suitable for X-ray diffraction were grown from a DCM solution layered with pentane. ^{1}H NMR (CD_2Cl_2 or CD_3CN): no resolvable peaks observed.^{19}F NMR (CD_2Cl_2): δ 18.1, −78.4.^{19}F NMR (CD_3CN): δ −77.3. MS (+FAB): *m*/*z* 1019 ([2M − OTf]$^+$), 435 ([M − OTf]$^+$), 231 ([M − Fe(OTf)$_2$]$^+$). Anal. Calcd (found) for $C_{14}H_{30}F_6FeN_4O_6S_2$: C, 28.78 (28.73); H, 5.17 (5.33); N, 9.59 (9.64). μ_{eff} (CD_2Cl_2) = 4.92μ_B.

Table 5. Crystallographic Data for Compounds [Fe(**3**)OTf$_2$] and [Fe(**5**)OTf]OTf[a]

	[Fe(**3**)OTf$_2$]	[Fe(**5**)OTf]OTf
chemical formula	$C_{18}H_{22}F_6FeN_4O_6S_2$	$C_{14}H_{30}F_6FeN_4O_6S_2$
fw	624.37	584.39
T (°C)	−70	20
space group	*Cc* (no. 9)	$P2_1/c$ (no. 14)
a (Å)	11.768(4)	11.248(7)
b (Å)	26.186(7)	13.345(6)
c (Å)	8.497(3)	16.345(11)
β (deg)	92.57(3)	95.17(6)
V (Å^3)	2615.8(15)	2444(2)
Z	4	4
ρ_{calcd} (g cm^{-3})	1.585	1.588
λ (Å)	0.71073	0.71073
μ (mm^{-1})	0.819	0.870
R1[b]	0.029	0.051
wR2[c]	0.066	0.106

[a] Siemens P4 diffractometer, graphite monochromated Mo Kα radiation, refinement based on F^2. [b] $R1 = \sum||F_o| - |F_c||/\sum|F_o|$. [c] $wR2 = \{\sum[w(F_o^2 - F_c^2)^2]/\sum[w(F_o^2)^2]\}^{1/2}$; $w^{-1} = \sigma^2(F_o^2) + (aP)^2 + bP$.

Crystallographic Details. Table 5 provides a summary of the crystallographic data for compounds [Fe(**3**)OTf$_2$] and [Fe(**5**)OTf]OTf. The absolute structure of [Fe(**3**)OTf$_2$] was determined by a combination of *R*-factor tests [$R_1^+ = 0.0293$, $R_{1-} = 0.0339$] and by use of the Flack parameter [$x^+ = +0.00(4)$, $x^- = +1.05(4)$]. (CCDC 256105 and 256106, respectively.)

Acknowledgment. We are grateful to BP Chemicals Ltd. for a CASE award to J.E. Mr. Richard Sheppard and Peter Haycock are thanked for their assistance in NMR measurements.

Supporting Information Available: Crystallographic data in cif format and molecular structures of [Fe(**3**)(OTf$_2$] and [Fe(**5**)(OTf)](OTf). This material is available free of charge via the Internet at http://pubs.acs.org.

IC0509229